

High Resolution, Rapid Flood Inundation Mapping for the U.S. National Water Model: From Forecast River Discharges to Forecast Inundation

Fernando Aristizabal^{1,2,3}, Fernando Salas³, Brian Avant^{1,3}, Bradford
Bates^{1,3}, Trevor Grout^{1,3}, Nick Chadwick^{1,3}, Zachary Wills^{1,3}, Gregory
Petrochenkov⁴, Roland Viger⁴, Jasmeet Judge²

¹Lynker Technologies, Boulder, CO, USA

²Center for Remote Sensing, University of Florida, Gainesville, FL, USA

³National Water Center, Office of Water Prediction, National Oceanic and Atmospheric Administration,
Tuscaloosa, AL, USA

⁴Water Mission Area, United States Geological Survey, Boulder, CO, USA

Key Points:

- KP1
- KP2
- KP3

Corresponding author: Fernando Aristizabal, fernando.aristizabal@noaa.gov

Abstract

Abstract here

Plain Language Summary

PLS here

1 Introduction

Flooding is one of the most significant natural disasters in the United States (US) affecting both the loss of life and property. In 2017 and 2019, river and flash flooding combined represented the leading cause of death among all natural disasters and second to deaths from heat wave in 2018 (National Weather Service, 2020b, 2019, 2018). More than an average of 104 deaths per year are attributed to flood events from the 10 year period ending in 2019 (National Weather Service, 2020a). Within that 10 year window, the most common activity victims were partaking in was driving when compared to other common activities leading to death (National Weather Service, 2020a). With respect to property damages, river and flash flooding have contributed to 60.7, 1.6, and 3.7 billion non-inflation adjusted US dollars in the annual periods of 2017 to 2019, respectively (National Weather Service, 2020b, 2019, 2018). The large spike in damages for 2017 can be attributed to the Hurricane Harvey event that primarily affected Texas in August. Unencouragingly, the trends related to flood damages and fatalities have been steadily increasing over recent decades. (Mallakpour & Villarini, 2015; Downton et al., 2005; Kunkel et al., 1999; Pielke Jr & Downton, 2000; Corringham & Cayan, 2019). Some are expecting that the hydrologic cycle will intensify which will lead to more extreme precipitation in some areas along with a greater risk of flooding (Tabari, 2020; Milly et al., 2002; Wing et al., 2018). Increasing trends in frequency and risk are not uniform across spatial regions with work by Slater and Villarini (2016) indicating that trends are increasing across the US Midwest/Great Lakes region while decreasing in coastal Southeast, Southwest and California.

Operational flood forecasting systems are primary tools in developing accurate forecasts for public awareness prior to life or property damaging events occur. One of these operational systems is the Advanced Hydrologic Prediction System (AHPS) maintained by National Oceanic Atmospheric Administration (NOAA) National Weather Service

(NWS) with approximately 3,781 forecast points across the US at typically short forecast horizons of 24 or 72 hours (McEnery et al., 2005). AHPS provides forecasting services in the form of ensemble stream flows at 3,781 forecast points illustrated in Figure 1 and flood inundation maps (FIM) at 188 of those forecast points shown in Figure 2. AHPS implements a series of advances including model calibration techniques (Z. Zhang, 2003; Hogue et al., 2003; Duan, 2003; Gupta et al., 2003; Parada et al., 2003), distributed modeling approaches (Reed et al., 2004; Koren et al., 2004; Duan & Schaake, 2002), ensemble forecasting (Day, 1985; Seo et al., 2000; Mullusky et al., 2002; Herr et al., 2002), enhanced data analysis procedures (McEnery et al., 2005), flood-forecasting inundation maps (Cajina et al., 2002), hydraulic routing models (Fread, 1973; Cajina et al., 2002), and multisensor precipitation techniques (Breidenbach et al., 1999; Kondragunta, 2001; Seo & Breidenbach, 2002; Bonnin, 1996). Despite the AHPS advances in operational flood forecasting, it lacks of sufficient spatial coverage and long-range forecast horizons. On an approximate basis, there is only one forecast point every 1,455 km of river and one forecast point with FIM every 29,261 km.

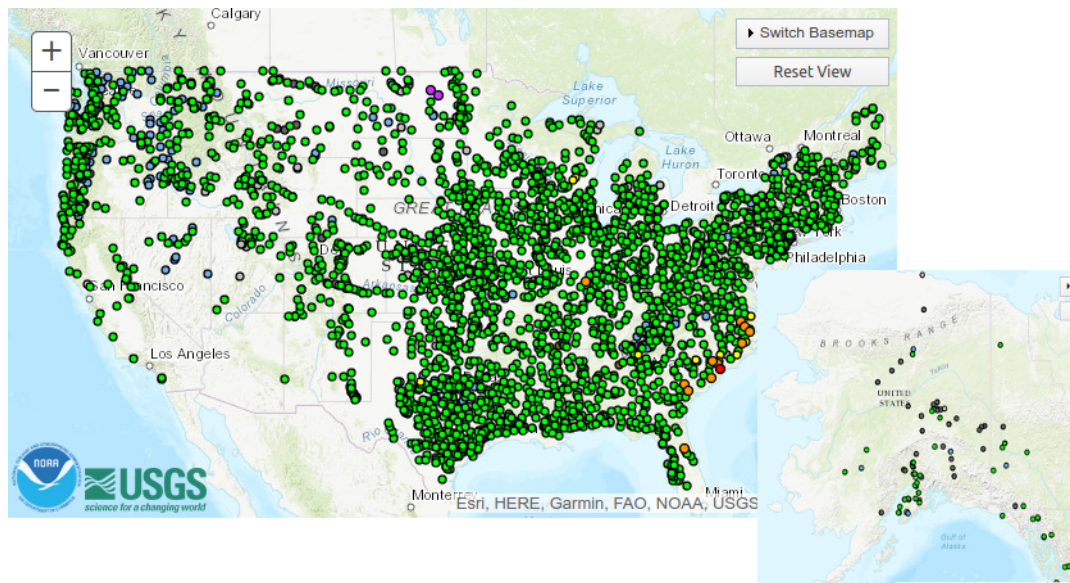


Figure 1. All 3,781 forecast points in United States' Advanced Hydrologic Prediction System for lower 48 states and Alaska. No forecast points in Hawaii or territories. From: water.weather.gov/ahps

Additional work is required to fill-in the gaps that the AHPS leaves in terms of spatial and temporal coverage. To broaden the forecasting domain, the Office of Water Pre-

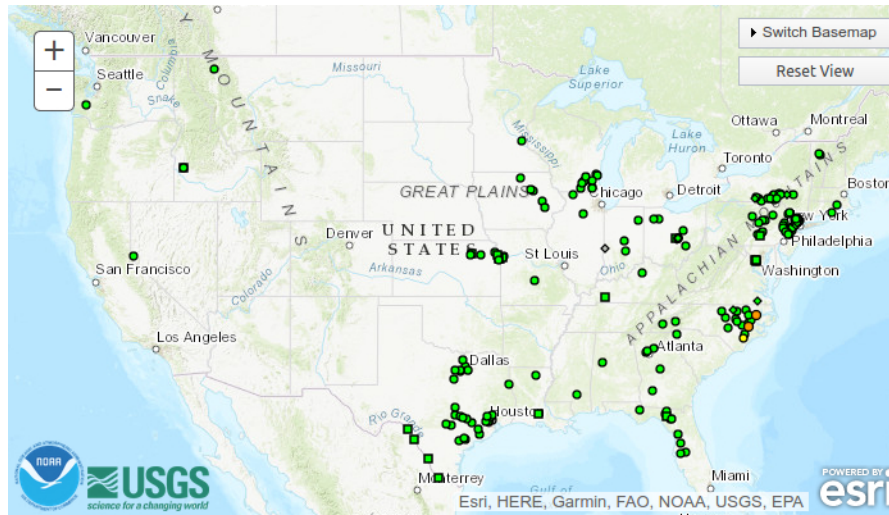


Figure 2. All 188 forecast points in United States’ Advanced Hydrologic Prediction System with flood inundation mapping capabilities. One forecast point near Juneau, Alaska not shown. No forecast points in Hawaii or remaining territories. From: water.weather.gov/ahps

diction (OWP) at the National Water Center (NWC) in Tuscaloosa, Alabama commissioned the development of the National Water Model (NWM) which is an instance of the Weather Research and Forecast Hydrologic Model (WRF-Hydro) (Gochis et al., 2018; Cosgrove et al., 2019). The NWM forecasts river discharges at more than 2.7 million forecast points at a variety of time horizons including some medium (10 day) and long (30 day) range forecast horizons. The NWM enhances but does not replace the spatial and temporal domain of the current AHPS capabilities at the 13 River Forecast Centers (RFC) in areas known as ‘hydro-blind’. It’s simply an additional model to be used in the forecasting and early warning decision making. Furthermore, the NWM as of V1.2 has implemented not only assimilation of real-time United States Geological Survey (USGS) stage discharges but also assimilation of flow forecasts from the AHPS forecast points which are in turn routed downstream and updated whenever a new point is reached. This configuration of the NWM is known as ‘Replace and Route’ or ‘RnR’ and is used to enhance the forecasting skill of the NWM with the best available regional-scale data.

The National Hydrography Dataset Plus (NHDPlus) version 2.1 is the basis for the hydrofabric in the NWM due to its comprehensive use with the hydrologic communities’ stakeholders (McKay et al., 2012). The term hydrofabric is used within the NWM jargon to describe the subset of hydrography comprised of geospatial datasets required for

hydrologic modeling including but not limited to stream networks, catchments, channel properties, and elevation data. The Muskingam-Cunge routing method is used within the NWM to reduce computational requirements of a continental scale model (Bedient et al., 2008; Ponce & Changanti, 1994; Gochis et al., 2018). Muskinham-Cunge routing scheme has been demonstrated by Cunge (1969) to be equivalent to the convective-diffusive wave method without consideration to wave dampening. As a result of high computational costs and large spatial domains, the need for high-resolution FIM at 10m or better requires additional post-processing from the principal output of the NWM which is forecast river discharges at the reach scale. The Height Above Nearest Drainage (HAND) terrain model is one such technique that can be used, along with synthetic rating curves (SRC), to convert riverine discharges to stages to inundation extents.

HAND normalizes topography along the nearest drainage path and its been demonstrated to be a good proxy and indicator of a series of important environmental conditions including soil environments, landscape classes, soil gravitational potentials, geomorphologies, soil moisture, and ground water dynamics (Rennó et al., 2008; A. Nobre et al., 2011). A. D. Nobre et al. (2016) showed evidence for utilizing the drainage normalizing HAND dataset as a proxy for flood potential to make static flood inundation maps from known stages. Zheng, Tarboton, et al. (2018) developed methodology for determining stage-discharge relationships known as synthetic rating curves (SRC) by sampling reach-averaged parameters from HAND datasets and inputting into the Manning’s equation (Gauckler, 1867; Manning et al., 1890). This collection of methods, coupling HAND with SRCs, has been experimented and compared to other sources of FIM including engineering scale models, in-situ observation, and remote sensing based observation with solid results in large spatial scale applications (Godbout et al., 2019; Johnson et al., 2019; Garousi-Nejad et al., 2019; A. D. Nobre et al., 2016; Afshari et al., 2018; Zheng, Maidment, et al., 2018; Teng et al., 2015, 2017; J. Zhang et al., 2018).

Many of those assessing HAND’s efficacy for producing FIM have noted opportunities for improvement. Godbout et al. (2019) found how reach length and slope are important parameters for maximizing mapping skill with the moderate values performing best. The colinearity of reach length and slope led Godbout et al. (2019) to propose that reaches of extreme lengths performed worse because of the extreme slope values, a parameter directly represented in Manning’s equation. Issues with the reach-average approaches have been documented in Tuozzolo et al. (2019) where large within reach vari-

ance of the roughness Manning’s n coefficient have been observed. These works motivate splitting junction to junction reaches into smaller and equidistant segments for better averaging behavior and SRC representation. Furthermore, Garousi-Nejad et al. (2019) noted improvements to mapping efficacy by conditioning monotonically decreasing thalweg elevations, adjusting the Manning’s n roughness coefficient, and using higher resolution (3m) DEM’s derived from light detection and ranging (Lidar). Use of higher resolution DEMs in that study was motivated by previous work with Lidar DEMs and least-cost thalweg derivations (Zheng, Maidment, et al., 2018). Further work by Johnson et al. (2019) noted the general under-prediction of HAND and suggested tuning the Manning’s n parameter to better align SRC’s with observations. Additionally, the sensitivity to low topographic relief and channel slope have been observed (Johnson et al., 2019; Godbout et al., 2019). Catchment boundary issues are noted where the interconnection of catchments are not properly accounted for (J. Zhang et al., 2018; McGehee et al., 2016). These findings suggesting improvements to HAND require advanced computational algorithms and software to compute a FIM hydrofabric required for producing continental-scale FIM (CFIM).

~~Thanks to the availability of~~ high-performance computing (HPC) and large scale high-resolution digital elevation models (DEM) such as the National Elevation Dataset (NED) at the 10m scale, HAND has been implemented into software for large-scale, continental computation. HAND was initially implemented into operational software by the National Flood Interoperability Experiment (NFIE) to generate FIM hydrofabric (will be used interchangeably with the datasets produced by HAND) rapidly on a high-performance computer (HPC) (Maidment, 2017; Y. Y. Liu et al., 2016). NFIE used open-source dependencies including the Terrain Analysis Using Digital Elevation Models (TauDEM) (Tarboton, 2005) and the Geospatial Data Abstraction Library (GDAL) (Warmerdam, 2008) to compute HAND for the Continental United States (CONUS) at 331 Hydrologic Unit Code (HUC) 6 processing units in 1.34 CPU years. By allocating 31 nodes at 20 cores per for a total of 620 available cores to the overall operation, it enabled the production to finish up in 36 hours consuming 3.2TB of peak memory and 5TB of total disk space. Originally, NFIE utilized the National Hydrography Dataset (NHD) Plus Medium Resolution (MR) to etch or burn flowlines prior to further conditioning but more recent work has advanced this to the more current NHDPlus High Resolution (HR) (Y. Liu et al., 2020). The original NFIE dataset was employed by the NWC to produce forecast

FIM from the NWM for use within its network of RFC's for additional guidance in hydro-blind regions and tagged as OWP's FIM V1.0. Further work by Djokic (2019), implemented a series of improvements to HAND including equi-distant reaches, updates to use with NHDPlusHR hydrography, and AGREE-DEM reconditioning (Hellweger & Maidment, 1997) into an ESRI Arc-Hydro workflow with use in ArcGIS and tagged as OWP FIM v2.0. More notably the software added the ability to derive drainage potentials on a per mainstem basis as originally conceptualized by (McGehee et al., 2016). Mainstem is generally used here as defined in Blodgett et al. (2020) but only available in mainstems downstream of forecast AHPS points within the workflow introduced by Djokic (2019). Overall, the software package is estimated to run CONUS at the full-resolution in 0.55 CPU years in a desktop setting.

To continue to innovate and implement the most advanced developments in FIM, the need arose to implement a more advanced software package with higher standards for specifications. The desired specifications were

1. Use easily accessible, open-source dependencies to promote free-use and open-access community development and research.
2. excellent single-core computational and memory performance with favorable, time and space complexities,
3. ability to parallelize across multiple cores and nodes within HPC or cloud compute environments,
4. preprocessing functionality within package pipeline to acquire and process input artifacts,
5. rapid inundation mapping capabilities to go from FIM hydrofabric datasets to forecast FIMs from NWM,
6. automated testing functionality to ensure modifications enhance forecast skill when compared to external sources,
7. ability to produce depth forecasts,
8. full NWM domain coverage (including Hawaii and Puerto Rico),
9. and improved FIM forecasting skill when compared to FIM v1.0 and v2.0.

To meet these higher specifications for the next generation of authoritative FIM capabilities, the OWP FIM V3.0 'Cahaba' was developed. It meets all the specifications

listed above including version on version improvement of FIM skill due to the implementation of new developments in HAND techniques. The following methods and results describe the work in more detail and demonstrates its efficacy in producing enhanced FIM from the NWM for operational forecast applications. Furthermore, it enables the contribution from the broader hydro-community as further advances are made in this developing area of research.

2 Materials and Methods

2.1 HAND

2.2 Synthetic Rating Curves

2.3 Evaluation and Testing

3 Data

4 Results

4.1 Computational Performance

5 Conclusions

Acknowledgments

Enter acknowledgments, including your data availability statement, here.

References

- Afshari, S., Tavakoly, A. A., Rajib, M. A., Zheng, X., Follum, M. L., Omranian, E., & Fekete, B. M. (2018). Comparison of new generation low-complexity flood inundation mapping tools with a hydrodynamic model. *Journal of Hydrology*, 556, 539–556.
- Bedient, P. B., Huber, W. C., Vieux, B. E., et al. (2008). *Hydrology and floodplain analysis*. Prentice Hall Upper Saddle River, NJ.
- Blodgett, D., Johnson, J. M., Sondheim, M., Wiczorek, M., & Frazier, N. (2020). Mainstems: A logical data model implementing mainstem and drainage basin feature types based on waterml2 part 3: Hy_features concepts. *Environmental Modelling & Software*, 104927.
- Bonnin, G. (1996). The noaa hydrologic data system. In *Preprints, 12th int. conf. on interactive information and processing system (iips) for meteorology*,

- 207 *oceanography, and hydrology, atlanta, ga, amer. meteor. soc* (pp. 410–413).
- 208 Breidenbach, J., Seo, D., Tilles, P., & Roy, K. (1999). Accounting for radar beam
209 blockage patterns in radar-derived precipitation mosaics for river forecast cen-
210 ters. In *Preprints, 15th int. conf. on interactive information and processing*
211 *systems (iips) for meteorology, oceanography, and hydrology, dallas, tx, amer.*
212 *meteor. soc* (Vol. 5).
- 213 Cajina, N., Sylvestre, J., Henderson, E., Logan, M., & Richardson, M. (2002). Fld-
214 view: The nws flood forecast mapping application. In *Proc. of the interactive*
215 *symp. on the advanced weather interactive processing system (awips)* (pp.
216 170–172).
- 217 Corringham, T. W., & Cayan, D. R. (2019). The effect of el niño on flood damages
218 in the western united states. *Weather, Climate, and Society*, 11(3), 489–504.
- 219 Cosgrove, B., Gochis, D., Graziano, T. M., Clark, E. P., & Flowers, T. (2019).
220 The evolution of noaa’s national water model: An overview of version 2.1 and
221 future operational plans. *AGUFM, 2019*, H51D–01.
- 222 Cunge, J. (1969). On the subject of a flood propagation computation method
223 (muskingum method). *Journal of Hydraulic Research*, 7(2), 205–230.
- 224 Day, G. N. (1985). Extended streamflow forecasting using nwsrfs. *Journal of Water*
225 *Resources Planning and Management*, 111(2), 157–170.
- 226 Djokic, D. (2019). *Arc hydro: Developing hand from nhdplushr and nwm data – de-*
227 *tailed workflow* (1st ed.). Environmental System Research Institute.
- 228 Downton, M. W., Miller, J. Z. B., & Pielke Jr, R. A. (2005). Reanalysis of us na-
229 tional weather service flood loss database. *Natural Hazards Review*, 6(1), 13–
230 22.
- 231 Duan, Q. (2003). Global optimization for watershed model calibration. *Calibration*
232 *of watershed models*, 6, 89–104.
- 233 Duan, Q., & Schaake, J. (2002). Results from the second international workshop on
234 model parameter estimation experiment (mopex). In *Paper presentation, sec-*
235 *ond federal interagency hydrologic modeling conf.*
- 236 Fread, D. L. (1973). Technique for implicit dynamic routing in rivers with tribu-
237 taries. *Water Resources Research*, 9(4), 918–926.
- 238 Garousi-Nejad, I., Tarboton, D. G., Aboutaleb, M., & Torres-Rua, A. F. (2019).
239 Terrain analysis enhancements to the height above nearest drainage flood

- 240 inundation mapping method. *Water Resources Research*, 55(10), 7983–8009.
- 241 Gauckler, P. (1867). *Etudes théoriques et pratiques sur l'écoulement et le mouvement*
 242 *des eaux*. Gauthier-Villars.
- 243 Gochis, D., Barlage, M., Dugger, A., FitzGerald, K., Karsten, L., McAllister, M., ...
 244 others (2018). The wrf-hydro modeling system technical description,(version
 245 5.0). *NCAR Technical Note*, 107.
- 246 Godbout, L., Zheng, J. Y., Dey, S., Eyselade, D., Maidment, D., & Passalacqua, P.
 247 (2019). Error assessment for height above the nearest drainage inundation
 248 mapping. *JAWRA Journal of the American Water Resources Association*,
 249 55(4), 952–963.
- 250 Gupta, H. V., Sorooshian, S., Hogue, T. S., & Boyle, D. P. (2003). Advances in au-
 251 tomatic calibration of watershed models. *Calibration of watershed models*, 6,
 252 9–28.
- 253 Hellweger, F., & Maidment, D. (1997). Agree-dem surface reconditioning system.
 254 *University of Texas, Austin*.
- 255 Herr, H., Welles, E., Mullusky, M., Wu, L., & Schaake, J. (2002). Simplified short
 256 term precipitation ensemble forecasts: Theory. In *Preprints, 16th conf. on hy-*
 257 *drology, orlando, fl, amer. meteor. soc., j1–j16*.
- 258 Hogue, T. S., Gupta, H. V., Sorooshian, S., & Tomkins, C. D. (2003). A multi-step
 259 automatic calibration scheme for watershed models. *Calibration of Watershed*
 260 *Models*, 6, 165–174.
- 261 Johnson, J. M., Munasinghe, D., Eyselade, D., & Cohen, S. (2019). An integrated
 262 evaluation of the national water model (nwm)–height above nearest drainage
 263 (hand) flood mapping methodology. *Natural Hazards and Earth System Sci-*
 264 *ences*, 19(11), 2405–2420.
- 265 Kondragunta, C. (2001). An outlier detection technique to quality control rain gauge
 266 measurements. *AGUSM*, 2001, H22A–07.
- 267 Koren, V., Reed, S., Smith, M., Zhang, Z., & Seo, D.-J. (2004). Hydrology labo-
 268 ratory research modeling system (hl-rms) of the us national weather service.
 269 *Journal of Hydrology*, 291(3-4), 297–318.
- 270 Kunkel, K. E., Pielke Jr, R. A., & Changnon, S. A. (1999). Temporal fluctuations in
 271 weather and climate extremes that cause economic and human health impacts:
 272 A review. *Bulletin of the American Meteorological Society*, 80(6), 1077–1098.

- 273 Liu, Y., Tarboton, D. G., & Maidment, D. R. (2020). *Height above nearest drainage*
274 *(hand) and hydraulic property table for conus* (Tech. Rep.). Oak Ridge Na-
275 tional Lab.(ORNL), Oak Ridge, TN (United States). Oak Ridge
- 276 Liu, Y. Y., Maidment, D. R., Tarboton, D. G., Zheng, X., Yildirim, A., Sazib, N. S.,
277 & Wang, S. (2016). A cybergis approach to generating high-resolution height
278 above nearest drainage (hand) raster for national flood mapping.
- 279 Maidment, D. R. (2017). Conceptual framework for the national flood interoper-
280 ability experiment. *JAWRA Journal of the American Water Resources Asso-*
281 *ciation*, 53(2), 245-257. Retrieved from [https://onlinelibrary.wiley.com/](https://onlinelibrary.wiley.com/doi/abs/10.1111/1752-1688.12474)
282 [doi/abs/10.1111/1752-1688.12474](https://onlinelibrary.wiley.com/doi/abs/10.1111/1752-1688.12474) doi: 10.1111/1752-1688.12474
- 283 Mallakpour, I., & Villarini, G. (2015). The changing nature of flooding across the
284 central united states. *Nature Climate Change*, 5(3), 250–254.
- 285 Manning, R., Griffith, J. P., Pigot, T., & Vernon-Harcourt, L. F. (1890). *On the flow*
286 *of water in open channels and pipes*.
- 287 McEnery, J., Ingram, J., Duan, Q., Adams, T., & Anderson, L. (2005). Noaa’s
288 advanced hydrologic prediction service: building pathways for better science
289 in water forecasting. *Bulletin of the American Meteorological Society*, 86(3),
290 375–386.
- 291 McGehee, R., Li, L., & Poston, E. (2016). The modified hand method. In
292 D. R. Maidment, A. Rajib, P. Lin, & E. P. Clark (Eds.), *National water center*
293 *innovators program summer institute report 2016* (Vol. 4).
- 294 McKay, L., Bondelid, T., Dewald, T., Johnston, J., Moore, R., & Rea, A. (2012).
295 *Nhdplus version 2: User guide; national operational hydrologic remote sensing*
296 *center: Washington, dc, 2012*.
- 297 Milly, P. C. D., Wetherald, R. T., Dunne, K., & Delworth, T. L. (2002). Increasing
298 risk of great floods in a changing climate. *Nature*, 415(6871), 514–517.
- 299 Mullusky, M., Wu, L., Herr, H., Welles, E., Schaake, J., Ostrowski, J., & Pryor,
300 N. (2002). Simplified short term precipitation ensemble forecasts: Applica-
301 tion. In *Preprints, 16th conf. on hydrology, orlando, fl, amer. meteor. soc., jp1*
302 (Vol. 19).
- 303 National Weather Service. (2018, Apr). *Summary of natural hazard statistics for*
304 *2017 in the united states*. NOAA. Retrieved from [https://www.weather.gov/](https://www.weather.gov/media/hazstat/sum17.pdf)
305 [media/hazstat/sum17.pdf](https://www.weather.gov/media/hazstat/sum17.pdf)

- 306 National Weather Service. (2019, Apr). *Summary of natural hazard statistics for*
 307 *2018 in the united states*. NOAA. Retrieved from [https://www.weather.gov/](https://www.weather.gov/media/hazstat/sum19.pdf)
 308 [media/hazstat/sum19.pdf](https://www.weather.gov/media/hazstat/sum19.pdf)
- 309 National Weather Service. (2020a, Nov). *Nws preliminary us flood fatality*
 310 *statistics*. NOAA's National Weather Service. Retrieved from [https://](https://www.weather.gov/arx/usflood)
 311 www.weather.gov/arx/usflood
- 312 National Weather Service. (2020b, Jun). *Summary of natural hazard statistics for*
 313 *2019 in the united states*. NOAA. Retrieved from [https://www.weather.gov/](https://www.weather.gov/media/hazstat/sum19.pdf)
 314 [media/hazstat/sum19.pdf](https://www.weather.gov/media/hazstat/sum19.pdf)
- 315 Nobre, A., Cuartas, L., Hodnett, M., Rennó, C., Rodrigues, G., Silveira, A., ...
 316 Saleska, S. (2011). Height above the nearest drainage – a hydrologically rele-
 317 vant new terrain model. *Journal of Hydrology*, 404(1), 13 - 29. Retrieved from
 318 <http://www.sciencedirect.com/science/article/pii/S0022169411002599>
 319 doi: <https://doi.org/10.1016/j.jhydrol.2011.03.051>
- 320 Nobre, A. D., Cuartas, L. A., Momo, M. R., Severo, D. L., Pinheiro, A., & Nobre,
 321 C. A. (2016). Hand contour: a new proxy predictor of inundation extent.
 322 *Hydrological Processes*, 30(2), 320–333.
- 323 Parada, L. M., Fram, J. P., & Liang, X. (2003). Multi-resolution calibration method-
 324 ology for hydrologic models: application to a sub-humid catchment. *Calibra-*
 325 *tion of Watershed Models*, 6, 197–212.
- 326 Pielke Jr, R. A., & Downton, M. W. (2000). Precipitation and damaging floods:
 327 Trends in the united states, 1932–97. *Journal of climate*, 13(20), 3625–3637.
- 328 Ponce, V. M., & Changanti, P. (1994). Variable-parameter muskingum-cunge
 329 method revisited. *Journal of Hydrology*, 162(3-4), 433–439.
- 330 Reed, S., Koren, V., Smith, M., Zhang, Z., Moreda, F., Seo, D.-J., & Participants,
 331 D. (2004). Overall distributed model intercomparison project results. *Journal*
 332 *of Hydrology*, 298(1-4), 27–60.
- 333 Rennó, C. D., Nobre, A. D., Cuartas, L. A., Soares, J. V., Hodnett, M. G., &
 334 Tomasella, J. (2008). Hand, a new terrain descriptor using srtm-dem: Mapping
 335 terra-firme rainforest environments in amazonia. *Remote Sensing of Environ-*
 336 *ment*, 112(9), 3469–3481.
- 337 Seo, D.-J., & Breidenbach, J. (2002). Real-time correction of spatially nonuniform
 338 bias in radar rainfall data using rain gauge measurements. *Journal of Hydrom-*

- eteorology, 3(2), 93–111.
- Seo, D.-J., Perica, S., Welles, E., & Schaake, J. (2000). Simulation of precipitation fields from probabilistic quantitative precipitation forecast. *Journal of Hydrology*, 239(1-4), 203–229.
- Slater, L. J., & Villarini, G. (2016). Recent trends in us flood risk. *Geophysical Research Letters*, 43(24), 12–428.
- Tabari, H. (2020). Climate change impact on flood and extreme precipitation increases with water availability. *Scientific Reports*, 10(1), 13768. Retrieved from <https://doi.org/10.1038/s41598-020-70816-2> doi: 10.1038/s41598-020-70816-2
- Tarboton, D. G. (2005). Terrain analysis using digital elevation models (taudem). *Utah State University, Logan*.
- Teng, J., Jakeman, A. J., Vaze, J., Croke, B. F., Dutta, D., & Kim, S. (2017). Flood inundation modelling: A review of methods, recent advances and uncertainty analysis. *Environmental Modelling & Software*, 90, 201–216.
- Teng, J., Vaze, J., Dutta, D., & Marvanek, S. (2015). Rapid inundation modelling in large floodplains using lidar dem. *Water Resources Management*, 29(8), 2619–2636.
- Tuozzolo, S., Langhorst, T., de Moraes Frasson, R. P., Pavelsky, T., Durand, M., & Schobelock, J. J. (2019). The impact of reach averaging manning’s equation for an in-situ dataset of water surface elevation, width, and slope. *Journal of Hydrology*, 578, 123866.
- Warmerdam, F. (2008). The geospatial data abstraction library. In *Open source approaches in spatial data handling* (pp. 87–104). Springer.
- Wing, O. E., Bates, P. D., Smith, A. M., Sampson, C. C., Johnson, K. A., Fargione, J., & Morefield, P. (2018). Estimates of present and future flood risk in the conterminous united states. *Environmental Research Letters*, 13(3), 034023.
- Zhang, J., Huang, Y.-F., Munasinghe, D., Fang, Z., Tsang, Y.-P., & Cohen, S. (2018). Comparative analysis of inundation mapping approaches for the 2016 flood in the brazos river, texas. *JAWRA Journal of the American Water Resources Association*, 54(4), 820–833.
- Zhang, Z. (2003). Hydrologic model calibration in the national weather service. *Calibration of watershed models*, 133.

- 372 Zheng, X., Maidment, D. R., Tarboton, D. G., Liu, Y. Y., & Passalacqua, P. (2018).
373 Geoflood: Large-scale flood inundation mapping based on high-resolution
374 terrain analysis. *Water Resources Research*, 54(12), 10–013.
- 375 Zheng, X., Tarboton, D. G., Maidment, D. R., Liu, Y. Y., & Passalacqua, P. (2018).
376 River channel geometry and rating curve estimation using height above the
377 nearest drainage. *JAWRA Journal of the American Water Resources Association*, 54(4), 785–806.
378